Department of Climate Change,
Energy, the Environment and Water

NSW Aridity index- High resolution (30 metre)

Background

The aridity index, also known as the Budyko radiative index of dryness, is a dimensionless parameter that represents the long-term balance between net radiation and precipitation (Nyman et al., 2014). The method used here to generate the high-resolution aridity index layer across New South Wales was developed by Nyman et al., 2014. Justification for the method is discussed in the method section below. The dataset allows identification of finer-scale variations in local moisture balance related to aspect owing to its 30 m resolution, unlike existing aridity index layers that are coarser resolution (~1 km; Trabucco and Zomer 2018; Zomer et al., 2022). This dataset can be used for assessing environmental conditions such as predicting the likelihood of debris flows after bushfires. The potential applications section discusses other possible uses of the aridity index.

Method for aridity index calculation

Aridity index or radiative index of dryness (AI_B) is a non-dimensional measure of the long-term balance between rainfall and net radiation (Nyman et al., 2014). Landscape aridity can be calculated from the ratio of the annual sum of net radiation and precipitation using the following equations and key datasets (Table 1).

Equation 1 $$AI_B = {}^{R_n}/_{\lambda \mathrm{P}}$$

where Rn is the annual sum of net radiation (MJ/m^2), a model of Australia's net radiation from Gallant et al (2014a) has been used here. P is the average daily rainfall (m/day), and λ is the latent heat of vaporisation (MJ/m^3) which is a function of topographic adjusted surface temperature, TD (°K) (Equations 2, 3, and 4).

Equation 2 $$\lambda = (3.146 - 0.002361\, T_D) \times 10^3$$

Equation 3

$$T_D\,(°\mathrm{C}) = T_a - \frac{\left(T_{lapse} \times (\mathrm{Z} - Z_b)\right)}{1000} + [k \times \left(S_{TD} - \frac{1}{S_{TD}}\right) \times \left(1 - \frac{LAI}{LAI_{max}}\right)]$$

Where, T_a = air temperature (°C), T_{lapse} = the change of temperature with elevation = 9.8 °C per thousand metres, STD = the topographic downscaling factor, a model of Australia's shortwave radiation ratio from Gallant et al (2014b) has been used here. Z = the elevation of each 30 m cell (elevation from SRTM), Z_b = the average elevation of 5 km tile (resampled STRM to 5 km), k = 1, and LAI = leaf area index of each 30 m cell, and LAI_{max} (resampled LAI to 5 km) = maximum leaf area index of each 5 km cell.

Equation 4

$$LAI = \frac{Band\ 5}{Band\ 4 + Band\ 6}$$

Due to the lack of ecological vegetation classes in NSW which were used by Nyman et al (2014) in Victoria, Landsat 8 bands were used to calculate LAI (Ganguly et al., 2012). Bands 4, 5, and 6 refer to Landsat 8 scenes bands.

Finally, for use in equation 2, $T_D\,(°\mathrm{C})$ is converted to degrees Kelvin (Equation 5).

Equation 5

$$T_D\,(°\mathrm{K}) = T_D\,(°\mathrm{C}) + 273$$

Table 1 parameters used for Aridity index calculations.

Parameter and symbol in the equation	Description	References
1 arc second monthly net radiation (R_n)	Modelled mean monthly solar radiation across Australia using topography from the 1 arcsecond resolution SRTM-derived DEM-S and climatic and land surface data. The twelve SRAD modelled net radiation layers (MJ/m^2/day) were used to calculate the net radiation layer.	Gallant et al. (2014a)
1 arc second monthly shortwave radiation ratio (S_{TD})	Modelled mean monthly shortwave radiation ratio across Australia using topography from the 1 arcsecond resolution SRTM-derived DEM-S and climatic and land surface data. The twelve SRAD	Gallant et al. (2014b)

	modelled short wave ratio layers were used to calculate the mean short wave ratio layer.	
Historical precipitation data (P)	Historical precipitation data from 1992 to 2021 was incorporated to calculate the mean daily rainfall.	Queensland Government, Australia Scientific Information for Land Owners-SILO.
Mean surface temperature (T_a)	Historical surface temperature data was incorporated to calculate the mean surface temperature over the 30 years between 1992 and 2021.	Queensland Government, Australia Scientific Information for Land Owners-SILO.
30-meter Shuttle Radar Topography Mission (SRTM) digital elevation model (Z)	SRTM elevation data was used to calculate topographic adjusted surface temperature.	NSW Government and DCCEEW 2019
30-meter Leaf Area Index (LAI)	Bands 4, 5 and 6 of 48 Landsat 8 scenes were used to create a Leaf Area Index layer by Equation 4.	United States Geological Survey (USGS)

Potential applications of the high-resolution aridity index dataset

Aridity index can be defined as the balance between rainfall and evaporative moisture demand. Aridity can have a significant influence over a range of ecosystem characteristics such as vegetation type, post-fire vegetation recovery rates, fuel moisture, and susceptibility to post-fire debris flows. The high-resolution aridity index dataset has a range of potential applications due to its high spatial resolution (30 m). Briefly discussed below are the relationships between aridity and landscape characteristics that may be of importance to land and water managers, to highlight the potential application of the aridity index dataset in environmental management decision-making.

Aridity and vegetation type

Aridity acts as a strong selective pressure for vegetation communities (Quiroga et al., 2010). Over long periods, plants compete for resources which leads to the development of distinct plant communities in different aridity zones (Berdugo et al., 2019). Vegetation type and structure is largely a function of aridity (Nyman et al., 2018; Figure 1). For example, there is a notable disparity in aridity values between dry and wet sclerophyll (Figure 1). The relationship between vegetation type and the 30 m resolution aridity index

dataset allows fine-scale assessments of potential habitat/vegetation refuges in areas where vegetation data is coarse or imprecise.

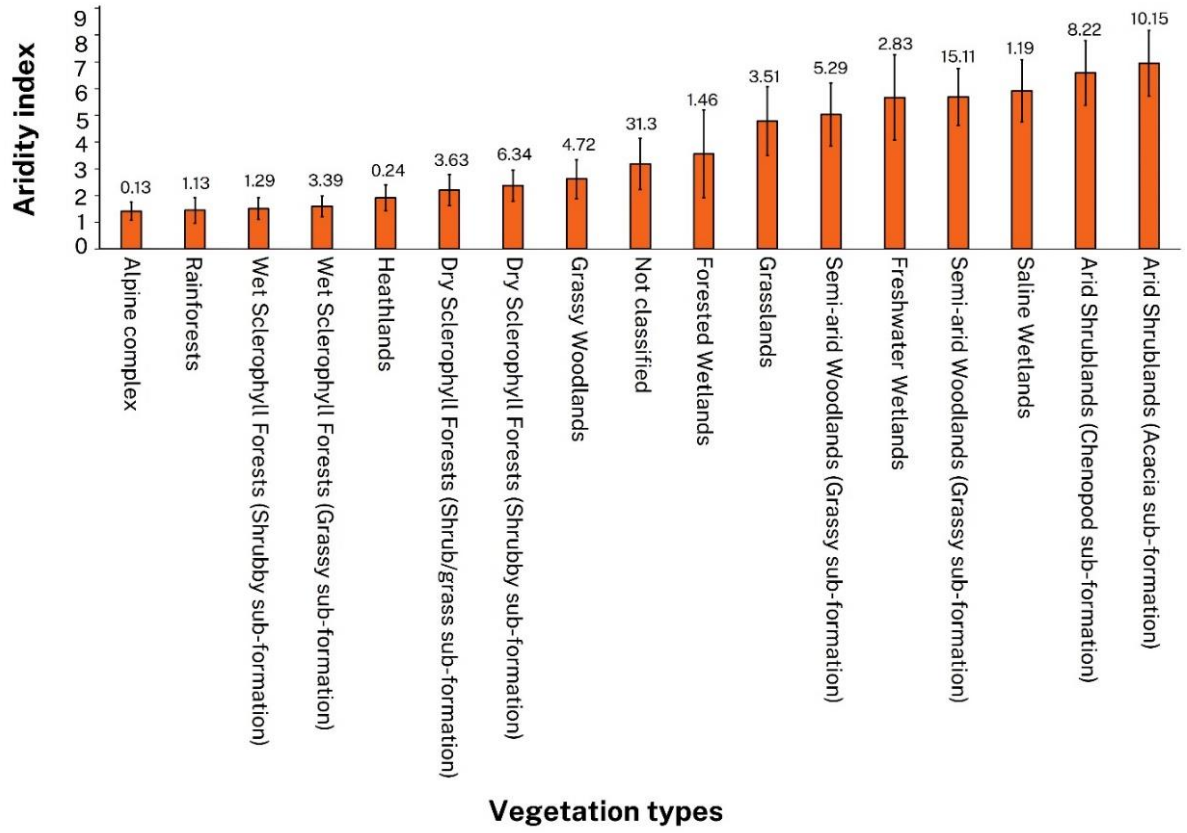

Figure 1 Mean aridity index values with standard error bars for different vegetation types within NSW. The labels on the bars indicate the proportion (%) of each vegetation type covering NSW.

Aridity and post-fire vegetation recovery

Aridity can affect plant recovery timeframes or regrowth rates following bushfires (Puig-Gironès et al., 2017). In arid environments, plant regrowth after fires typically takes longer compared to more humid areas. The slow pace of recovery can be due to the combined effects of surface dryness (Shuang and Christopher 2012), severity, temperature, and duration of fires (Manges et al., 2021). A comparison of Normalized Difference Vegetation Index (NDVI) as a proxy for vegetation recovery over time (Zhou et al., 2023) versus different aridity categories in the Tuross River catchment indicates that dryness is a crucial factor in vegetation recovery (Figure 2). Regrowth in the 3 years after the 2019/2020 fires was significantly slower where aridity is greater than ~2. The relationship between average NDVI and aridity shows a negative trend beyond the second quartile, as depicted in Figure 2, where aridity values exceeded approximately ~ 2. The significant differences observed between aridity quartiles (Table A4) lend support to the notion that

higher levels of aridity will lead to slower vegetation regrowth. However, this is complicated by the fact that vegetation in drier areas may tend to have lower NDVI values. Nonetheless, this highlights the potential applicability of the NSW aridity index dataset for prioritising and monitoring post-fire vegetation recovery.

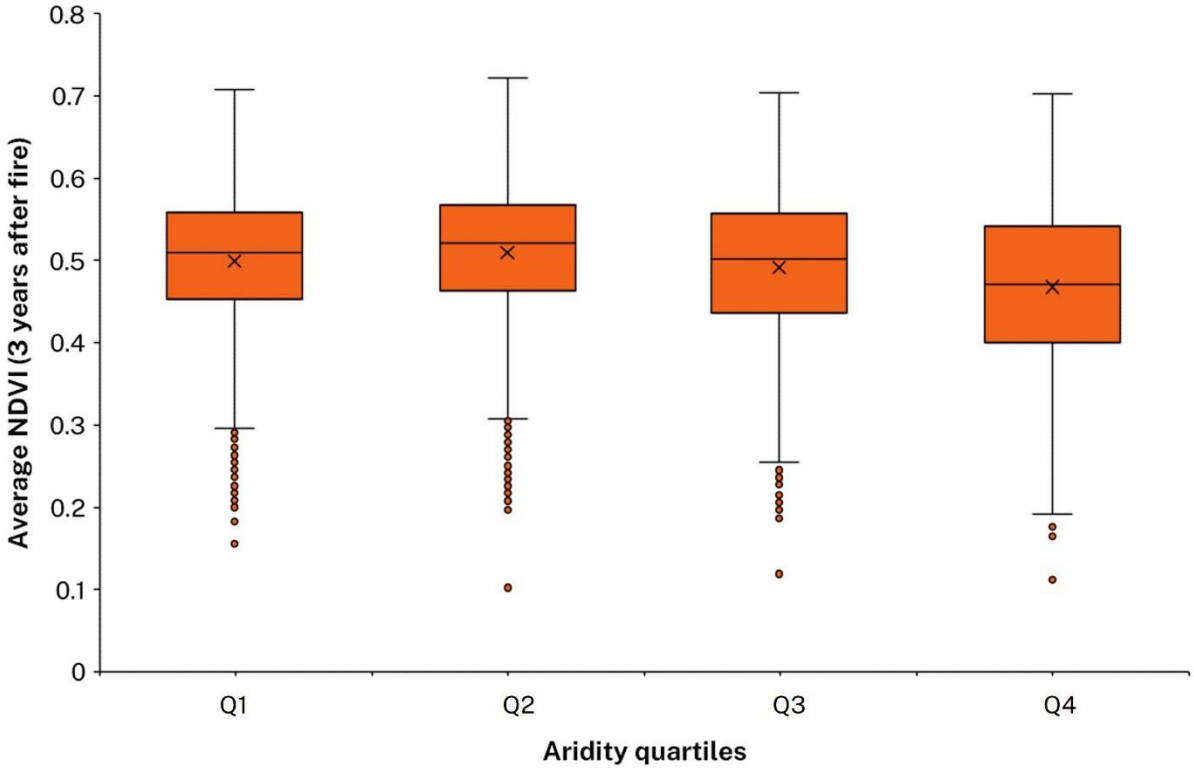

Figure 2 The average Normalised Difference Vegetation Index (NDVI) 3 years after 2019-2020 bushfire against aridity index quartile groups in Tuross River catchment area. Each aridity quartile group represents a range of aridity values:Q1 = 0.106539-1.540778, Q2 = 1.540779-1.853088, Q3 = 1.853089-2.099244, Q4 = 2.099245-2.716552. The Kruskal Wallis test and the post-hoc pairwise comparison tests showed a significant difference between NDVI values against each aridity quartile groups (see Table 2).

Table 2 Description of applied statistical tests.

Statistical test	P-value	Null hypothesis	Description
Kolmogorov Smirnov test[a]	< 0.05	normally distribution of variable — average NDVI	The null hypothesis is rejected when the p-value is less than 0.05. As a result, the dependent variable (NDVI) does not have a normal distribution (see Table A1).
Leven's test[a]	< 0.05	Homogeneity of variances of variable within groups — average NDVI in aridity quartiles	The null hypothesis is rejected when the p-value is less than 0.05. As a result, NDVI variances are not uniformly distributed in aridity quartile groups (see Table A2).
[b]Kruskal Wallis test	< 0.05	The same distribution of variable within groups — average NDVI in aridity quartiles	The null hypothesis is rejected when the p-value is less than 0.05. As a result, the distribution of the dependent variable (NDVI) in the aridity quartile groups differs (see Table A3).
Post-hoc pairwise comparison — Dunn Bonferroni test	< 0.05	The same distribution of variable within groups — average NDVI in aridity quartiles	The null hypothesis is rejected for all pairwise comparison of NDVIs in aridity quartiles (1-4). As a result, the distribution or median ranks of the dependent variable (NDVIs) in all pairwise aridity quartile groups differ (see Table A4).

[a]Assumptions for one-way Anova are violated (normality distribution and homogeneity of variances), one-way ANOVA test is not recommended.

[b]The Kruskal-Wallis test was used as an equivalent non-parametric test of one-way ANOVA.

Aridity and fuel moisture

Aridity has an influence on fuel moisture whereby ground fuel in wetter areas dries slower compared to drier parts of the landscape (Nyman et al., 2018). More research is required to understand this relationship, but the implications are that wetter parts of the landscape may act as barriers to landscape flammability by reducing the connectivity of dry surface fuel (Nyman et al., 2018). In severe drought conditions however, this influence is likely to be muted. Evidence from the 2019/2020 bushfires indicates that prolonged dry periods can reduce fuel moisture across landscapes and different vegetation types, meaning that these 'wetter' barriers may not persist in extremely dry conditions (Deb et al., 2020; Ehsani et al., 2020).

Aridity and post-fire debris flows

Aridity is one of the significant factors that play a major role in post-fire debris flow activity (Nyman et al., 2015). Through its influence on soil hydraulic properties, aridity has been shown to be an important factor determining the susceptibility of hillslopes to severe post-fire erosion (Sheridan et al. 2015; Moody et al., 2013). Locally drier slopes – equator-facing slopes for example – have been shown to have lower infiltration rates and the post-fire vegetation recovery is slower than polar-facing slopes with higher average moisture balances, allowing a longer window within which a high-intensity rainfall event can trigger severe erosion (Noske et al., 2016). In applying this high-resolution aridity layer, alongside other key factors that influence debris flow, namely slope, fire severity, geology and soil erodibility, have been used to produce a NSW post-fire debris flow map (NSW Government and NSW DCCEEW 2024).

References

Berdugo, M., Maestre, F.T., Kéfi, S., Gross, N., Le Bagousse-Pinguet, Y. and Soliveres, S., 2019. Aridity preferences alter the relative importance of abiotic and biotic drivers on plant species abundance in global drylands. *Journal of Ecology*, *107*(1), pp.190-202. *https://doi.org/10.1111/1365-2745.13006.*

Gallant, John; Austin, Jenet; Van Niel, Tom (2014a): Mean monthly net radiation modelled using the 1" DEM-S - 1" mosaic. v2. CSIRO. Data Collection. https://doi.org/10.4225/08/57980D45BC556.

Gallant, John; Austin, Jenet; Van Niel, Tom (2014b): Mean monthly shortwave radiation ratio modelled using the 1" DEM-S - 1" mosaic. v2. CSIRO. Data Collection. https://doi.org/10.4225/08/5799D4A672AFF.

Ganguly, S., Nemani, R.R., Zhang, G., Hashimoto, H., Milesi, C., Michaelis, A., Wang, W., Votava, P., Samanta, A., Melton, F. and Dungan, J.L., 2012. Generating global leaf area index from Landsat: Algorithm formulation and demonstration. Remote Sensing of Environment, 122, pp.185-202. https://doi.org/10.1016/j.rse.2011.10.032.

Menges, E.S., Smith, S.A., Clarke, G.L. and Koontz, S.M., 2021. Are fire temperatures and residence times good predictors of survival and regrowth for resprouters in Florida, USA, scrub?. *Fire Ecology*, *17*, pp.1-12. https://doi.org/10.1186/s42408-021-00101-8.

Moody, J.A., Shakesby, R.A., Robichaud, P.R., Cannon, S.H. and Martin, D.A., 2013. Current research issues related to post-wildfire runoff and erosion processes. *Earth-science reviews*, 122, pp.10-37. https://doi.org/10.1016/j.earscirev.2013.03.004.

Noske, P.J., Nyman, P., Lane, P.N. and Sheridan, G.J., 2016. Effects of aridity in controlling the magnitude of runoff and erosion after wildfire. *Water Resources Research*, *52*(6), pp.4338-4357. https://doi.org/10.1002/2015WR017611.

Nyman, P., Sherwin, C.B., Langhans, C., Lane, P.N. and Sheridan, G.J., 2014. Downscaling regional climate data to calculate the radiative index of dryness in complex terrain. *Australian Meteorological and Oceanographic Journal*, *64*(2), pp.109-122. https://doi.org/10.1071/ES14011.

Nyman, P., Baillie, C.C., Duff, T.J. and Sheridan, G.J., 2018. Eco-hydrological controls on microclimate and surface fuel evaporation in complex terrain. *Agricultural and Forest Meteorology*, *252*, pp.49-61. https://doi.org/10.1016/j.agrformet.2017.12.255.

Nyman, P., Smith, H.G., Sherwin, C.B., Langhans, C., Lane, P.N. and Sheridan, G.J., 2015. Predicting sediment delivery from debris flows after wildfire. *Geomorphology*, 250, pp.173-186.

Puig-Gironès, R., Brotons, L. and Pons, P., 2017. Aridity influences the recovery of vegetation and shrubland birds after wildfire. *PloS one*, 12(3), p.e0173599. https://doi.org/10.1371/journal.pone.0173599.

Queensland Government, Australian climate data from 1889 to yesterday, accessed form Australia Scientific Information for Land Owners-SILO, Data Portal [SILO | LongPaddock | Queensland Government], date accessed 2023-03-10.

Quiroga, R.E., Golluscio, R.A., Blanco, L.J. and Fernández, R.J., 2010. Aridity and grazing as convergent selective forces: an experiment with an Arid Chaco bunchgrass. *Ecological Applications*, *20*(7), pp.1876-1889. https://doi.org/10.1890/09-0641.1.

Sheridan GJ, Nyman P, Langhans C, Cawson J, Noske PJ, Oono A, Van der Sant R and Lane PNJ (2015) 'Is aridity a high-order control on the hydro–geomorphic response of burned landscapes?', *International Journal of Wildland Fire*, 25(3):262–267, doi: 10.1071/WF14079.

Shuang, L. and Christopher, P., 2012. Vegetation regrowth trends in post forest fire ecosystems across North America from 2000 to 2010. *Natural Science*, 2012. DOI:10.4236/ns.2012.410100.

State Government of NSW and NSW Department of Climate Change, Energy, the Environment and Water 2019, SRTM DEM derived 18 degree or greater - SRTM18, accessed from The Sharing and Enabling Environmental Data Portal [https://datasets.seed.nsw.gov.au/dataset/362d69f3-d3d5-4e10-959c-97c1c63935e3], date accessed 2023-03-10.

State Government of NSW and NSW Department of Climate Change, Energy, the Environment and Water 2024, NSW post-fire debris flow susceptibility map, accessed from The Sharing and Enabling Environmental Data Portal [https://datasets.seed.nsw.gov.au/dataset/f4b9f20a-65d5-4b64-8803-55c8beb1a67d], date accessed 2024-04-18.

Trabucco, A. and Zomer, R.J., 2018. Global aridity index and potential evapotranspiration (ET0) climate database v2. *CGIAR Consort Spat Inf, 10,* p.m9.

United States Department of the Interior, accessed form United States Geological Survey-USGS. Data Portal [EarthExplorer (usgs.gov)], date accessed 2023-03-10.

Zomer, R.J., Xu, J. and Trabucco, A., 2022. Version 3 of the global aridity index and potential evapotranspiration database. *Scientific Data, 9*(1), p.409. https://doi.org/10.1038/s41597-022-01493-1.

Zhou, D., Zhang, L., Hao, L., Sun, G., Xiao, J. and Li, X., 2023. Large discrepancies among remote sensing indices for characterizing vegetation growth dynamics in Nepal. *Agricultural and Forest Meteorology, 339,* p.109546. https://doi.org/10.1016/j.agrformet.2023.109546.

Appendix

Table A1 test of normality with Kolmogorov-Smirnov.

Average NDVI	Statistic	df[a]	Sig.[b]
Quartile 1 & 2	0.048	15678	< 0.001

[a]df = degree of freedom

[b]Sig. = Significance difference

Table A2 Homogeneity of variances with Levene's test.

		Levene Statistic	df1	df2	Sig.
Average NDVI	Based on Mean	76.699	3	15674	< 0.001
	Based on Median	77.795	3	15674	< 0.001
	Based on Median and with adjusted df	77.795	3	15581.108	< 0.001
	Based on trimmed mean	78.313	3	15674	< 0.001

Table A3 Kruskal-Wallis test.

	Average NDVI
Kruskal-Wallis H	442.635
df	3
Sig.	< 0.001

Table A4 Pairwise comparison of average NDVI within aridity quartile groups.

Pair groups	P-value	Test statistic	Standard Error	Standard test statistic
Quartile 1 & 2	< 0.001	-566.324	104.695	-5.409
Quartile 1 & 3	< 0.001	360.422	102.476	3.517
Quartile 1 & 4	< 0.001	1515.680	104.131	14.555
Quartile 2 & 3	< 0.001	926.747	100.644	9.208
Quartile 2 & 4	< 0.001	2082.005	102.330	20.346
Quartile 3 & 4	< 0.001	1155.258	100.057	11.546